PROBABILISTIC RISK ANALYSIS AND MARGIN PROCESS FOR A FLEXIBLE THERMAL PROTECTION SYSTEM

Steven A. Tobin, Andrew J. Brune, and Angela L. Bowes

NASA Langley Research Center

ABSTRACT

Atmospheric entry vehicle thermal protection systems are margined due to the uncertainties that exist in entry aeroheating environments and the thermal response of the materials and structures. Entry vehicle thermal protections systems are traditionally over-margined for the heat loads that are experienced along the entry trajectory by designing to survive stacked worst-case scenarios. Additionally, the conventional heat shield design and margin process offers very little insight into the risk of over-temperature during flight and the corresponding reliability of the heat shield performance. A probabilistic margin process can be used to appropriately margin the thermal protection system based on rigorously calculated risk of failure. This probabilistic margin process allows engineers to make informed aeroshell design, entry-trajectory design, and risk trades while preventing excessive margin from being applied. This study presents the methods of the probabilistic margin process and how the uncertainty analysis is used to determine the reliability of the entry vehicle thermal protection system and associated risks of failure.

1. INTRODUCTION

Potential missions have been identified that will require a planetary entry system to have an aeroshell much larger in diameter than the diameter of any feasible launch vehicle [1]. These missions include high-altitude landings on Mars and landing high mass payloads on Earth and other planets or moons with an atmosphere. NASA has been developing the Hypersonic Inflatable Aerodynamic Decelerator (HIAD) to use as a potential entry system for these applications. An inflatable heatshield can be packed and stowed to fit within current launch vehicle shroud sizes and then deployed (inflated) prior to atmospheric entry resulting in a heatshield much larger than the stowed diameter, providing increased mission capability in terms of drag generation. This allows for increased flexibility in landing location or additional payload capability. Due to the high heat loads encountered in hypersonic atmospheric entry environments, the inflatable aeroshell of a HIAD entry system relies on a layered blanket flexible thermal protection system (FTPS) to prevent the underlying stacked toroid inflatable structure (IS) from exceeding its thermal limits. **Figure 1** depicts an example HIAD.

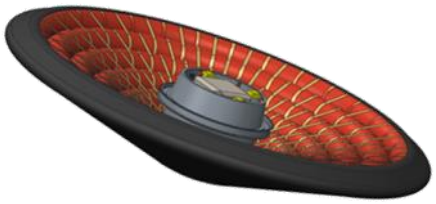

Figure 1. Experimental HIAD Reentry Vehicle

FTPS materials and layups have undergone extensive aerothermal arc jet testing in a stagnation configuration to evaluate thermal performance and provide boundary condition and in-depth temperature measurement data for thermal model correlation and validation [1]. The general FTPS material layup is shown in **Figure 2**, which displays numbered interfaces in between the layers. The outer fabric protects the underlying insulation layers from being directly exposed to the incident convective heat flux and the aerodynamic shear forces. The outer fabric also protects the underlying insulation layers from the abrasion and mechanical forces associated with packing and deploying. The insulator layers reduce thermal soak back and the gas barrier prevents hot gas impingement on to the underlying IS.

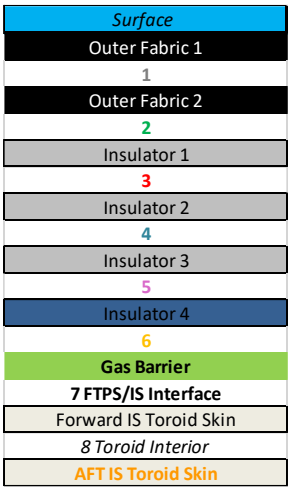

Figure 2. General FTPS Layup

The Low Earth Orbit Flight Test of an Inflatable Decelerator (LOFTID) is a demonstration flight project that will be used to validate computational models and advance understanding of the HIAD technology. Since the LOFTID project is an experimental flight, the desire is to drive the FTPS and IS in the entry environment to temperatures that cover a large range of applicability to the thermal response models used. This will allow the thermal response models to be better improved and validated post-flight using LOFTID's extensive instrumentation embedded within the aeroshell.

Entry vehicle heat shields are typically over-sized for the heat loads that are experienced along the entry trajectory by designing to survive stacked worst-case scenarios. Additionally, the conventional heat-shield design and margin process offers very little insight into the risk of over-temperature during flight and the corresponding reliability of the heat shield performance [2]. A probabilistic margin process allows engineers to make informed aeroshell design, entry-trajectory design, and risk trades while preventing excessive margin from being applied [3,4]. This paper describes the methodology used to carry out a probabilistic margin process and the resulting calculation of the risk of aeroshell over-temperature and the corresponding reliability of successful FTPS performance. The paper explains how this risk calculation is used to size the FTPS for LOFTID and establish flight allowable entry heat load constraints.

2. CRITICAL AEROSHELL THERMAL RESPONSE AND MARGIN PROCESS

This section provides an overview and the objectives of the probabilistic RV aeroshell margin process.

2.1 Aeroshell Thermal Response Overview

The LOFTID reentry vehicle's (RV) FTPS protects the aeroshell IS forebody from over-heating during atmospheric entry. For a given FTPS size and entry trajectory, critical FTPS and IS temperatures in response to entry heat loads must be predicted in order to prescribe the FTPS thickness and determine a corresponding flight allowable entry heat load. **Figure 3** shows the external heating drivers on the RV during atmospheric entry. Note that the bulk of the aft-body is not covered by FTPS and the aft-side toroid skin is directly expose to wake convective heating during entry.

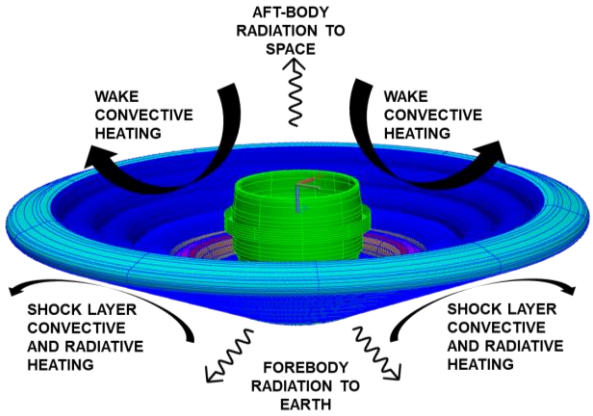

Figure 3. RV Thermal Model Geometry (Thermal Desktop) with External Heating

The primary critical temperature prediction is the maximum FTPS/IS interface (IF) temperature, where the FTPS gas barrier touches the IS on the aeroshell forebody flank. The location of the FTPS/IS interface is shown in **Figure 2** as interface 7. Another critical aeroshell temperature prediction is the maximum aft side IS toroid skin temperature, where the toroid is exposed directly to wake heat loads. **Figure 4** depicts locations on the aeroshell where temperatures are predicted for atmospheric entry. Points 1 and 2 in the figure are the two critical thermal analysis locations mentioned. The FTPS layup shown in **Figure 2** is located at Point 1 in **Figure 4.**

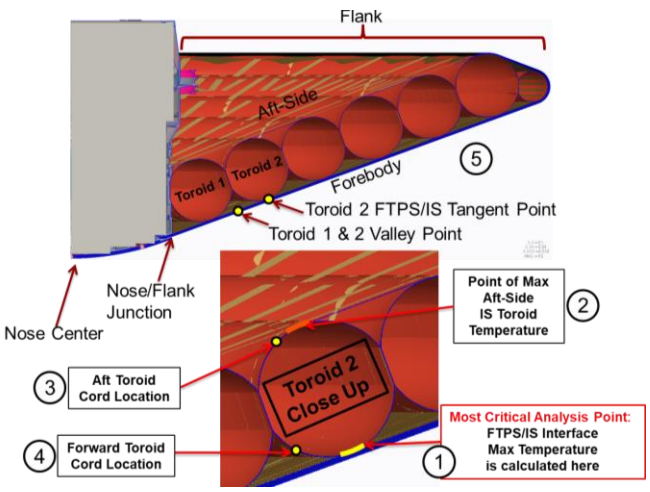

Figure 4. Aeroshell Critical Thermal Analysis Locations

2.2 Probabilistic Margin Process

There is uncertainty in the critical temperature predictions due to the uncertainties that exist in atmospheric entry aeroheating environments, the thermal response of the FTPS/IS materials, as wells as the thermal limits of the

materials. These uncertainties are mitigated by tailoring the planned entry heat load and the FTPS thickness and applying temperature limit safety deltas in order to apply margin to the FTPS/IS critical temperature predictions. The initial entry state (entry velocity, flight path angle, and entry mass) determines the expected atmospheric entry conditions and resulting heat load that the RV will experience. Since there is some flexibility in the LOFTID RV's initial entry state, this process can be used to select an appropriate combination of entry state parameters and FTPS size that allows the aeroshell to survive entry with the desired level of reliability.

The probabilistic margin process used to calculated the reliability of the aeroshell is carried out by an uncertainty analysis method which employs an end-to-end Monte Carlo simulation (discussed in **Section 3**). The end-to-end Monte Carlo simulation propagates the uncertainties in the trajectory and aeroheating model into the FTPS and RV thermal models to quantify the resulting probability distribution of the FTPS/IS thermal response, more specifically, the maximum critical temperatures at locations 1 and 2 in **Figure 4**.

LOFTID's aeroshell reliability standard dictates the goal that the aeroshell be margined such that there is at least a 97.7% chance of survival. This means it is desired that the critical aeroshell temperatures have less than 2.3% chance of exceeding their allowable temperatures. The calculated maximum critical temperature probability distributions are used to determine the expected maximum critical temperatures (**T_Exp**) and the probabilities of exceeding their flight allowable temperatures (**T_Allow**) for a particular FTPS size and nominal entry heating profile. Additionally, the maximum critical temperatures at which there is a 97.7% chance of not exceeding is calculated (**T_97.7_Calc**). For example, if the maximum FTPS/IS interface probability distribution shows that there is a 97.7% chance of not exceeding 405°C, then T_97.7_Calc is defined as 405°C.

The flight allowable temperature is defined as a critical component's upper temperature limit (**T_Limit**) minus a safety temperature delta (**T_Safe**). The safety delta is a knock-down on T_Limit that accounts for structural uncertainty in thermal model not validated by ground test (aft-side toroid skin thermal response model), ground test to flight applicability, uncertain parameters that are not taken into account in the probabilistic uncertainty analysis process or have inaccurate probability distributions, and unknown-unknowns in general. **Table 1** lists the maximum interface temperature thermal performance parameters that are used to determine the flight allowable temperatures.

Table 1. Thermal Performance Parameters

Parameter	FTPS/IS IF	Toroid Skin
T_Limit	400°C	480°C
T_Safe	5°C	20°C
T_Allow	395°C	460°C

The **performance margin** is defined as the difference between the expected maximum critical temperature and its *allowable* temperature (T_Allow – T_Exp). In order to margin the aeroshell according to LOFTID's reliability standard, the FTPS and entry heating profile should be tailored so that the critical aeroshell temperatures are calculated to have less than or equal to 2.3% of exceeding their allowable temperatures. In other words, the performance margin should be greater than or equal to the temperature difference between T_Exp and T_97.7_Calc. The **performance margin deficit** indicates approximately how much more performance margin is needed to satisfy the reliability standard and is calculated as T_97.7_Calc – T_Allow.

Figure 5 displays a notional visualization of the performance margin, performance margin deficit, and the thermal performance parameters (T_Allow, T_Limit, and T_Safe) relative to the calculated nominal (**T_Nom**) and expected maximum critical temperatures. The offset between the nominal and expected maximum critical temperature prediction and is primarily due to the model error bias (discussed in **Section 3**). The bell curve in **Figure 5** represents an idealized histogram of maximum critical temperature dispersions resulting from an end-to-end Monte Carlo simulation.

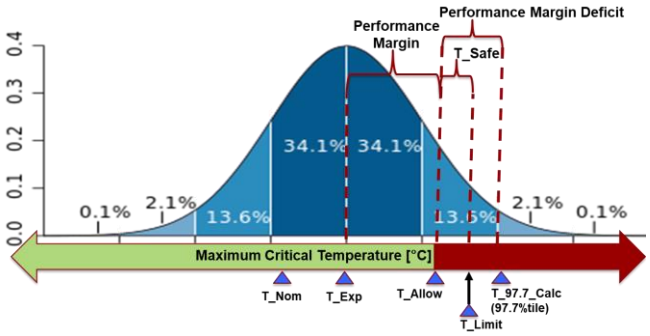

Figure 5. Example Maximum Critical Temperature Probability Distribution

The performance margin deficit can be eliminated by taking measures to lower the expected interface temperature, which results in moving T_97.7_Calc to the left. This can be accomplished by modifying the nominal entry state to decrease the nominal entry heat load, reducing conservatism in the thermal response models, or adding thermal protection to the aeroshell. The FTPS thickness can only be adjusted in increments of the thickness of a layer of insulation, which causes relativity large changes in the expected interface temperature. Altering the nominal entry heat load can more finely tune the expected interface temperature. The amount of fine tuning available comes from the performance capabilities of the upper stage orbit transfer

vehicle and must be balanced with primary payload launch window margins and payload mass.

3. UNCERTAINTY PROPAGATION APPROACH

In the previous section, the critical aeroshell performance locations were defined and the margin process and definitions were described. This section discusses the uncertainty propagation approach to quantify the distribution of maximum interface temperature for between the IS and FTPS.

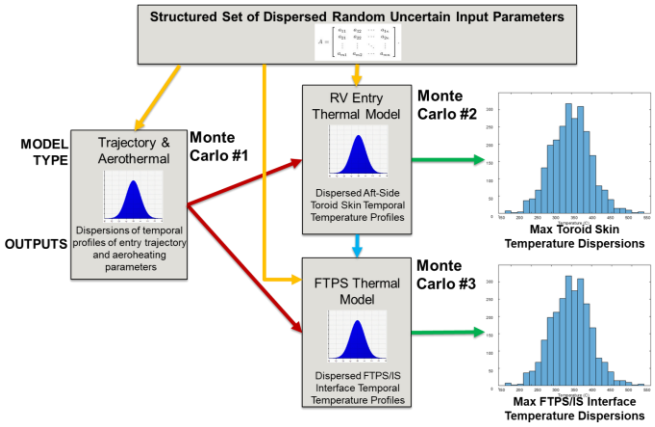

Figure 6. Uncertainty analysis process using the end-to-end Monte Carlo simulation approach.

As noted in the previous section, an end-to-end Monte Carlo process is used to propagate the uncertainty in the trajectory, aerothermal, and thermal models to quantify the uncertainty in the maximum interface temperature between the FTPS and IS, as shown in **Figure 6.** The process begins with generating a structured set of samples that include uncertain parameters from each of the model disciplines, including trajectory, aerothermodynamics, and thermal. The uncertain parameters are then propagated through the computational models of the respective disciplines. Each discipline provides output, or linking variables, which are required for input to another discipline. For example, the desired uncertain output from the trajectory model, given trajectory-specific uncertain parameter inputs, are the temporal profiles of atmospheric quantities (i.e., density) and velocity. These temporal profiles are provided as an input to the aerothermodynamics model. The process is repeated for the thermal models, which finally results in the dispersion of FTPS/IS interface and toroid skin temperature temporal profiles. The maximum of these critical temperatures is then extracted from the respective set of temporal profiles to construct a histogram of the maximum interface temperature and maximum toroid skin temperature as a performance quantities of interest. The details associated with each of the components in **Figure 6** are described further in the following subsections.

3.1 Sample Generation

A set of 2000 samples are generated for a total of 74 uncertain variables, which are inputs to either the trajectory, aerothermal, or thermal models, using Latin Hypercube structured sampling [5]. Latin Hypercube sampling has been used since the 1970's for Monte Carlo studies as a technique for reducing the required number of samples to converge in statistics of a desired output. The approach is to sample from the domain using partitions based on the probabilistic distribution of each uncertain input variable, rather than the common practice to randomly sample based on the probabilistic distribution alone for each of the uncertain input variables. Partitioning of the uncertain sample space allows for sampling near the domain boundaries, which corresponds to the upper and lower bounds of the uniformly distributed variables and the tails of normally distributed variables.

Each of the 2000 samples corresponds to 2000 trajectories with each having a unique set of trajectory, aerothermal, and thermal uncertain input variables. Uncertainties in vehicle and entry conditions used in the trajectory models define the trajectories. Each trajectory is assigned scale factors for constructed aerothermal indicators. Each trajectory is also assigned a set of thermal uncertain variables. The characterization of these uncertain parameters are explained for each discipline, including assumptions for the models used, in the next few subsections.

3.2 Trajectory Models and Uncertainties

The Program to Optimize Simulation Trajectories II (POST2) is used to compute the trajectories for the end-to-end Monte Carlo study. POST2 simulates six degree-of-freedom environments, beginning at initial conditions and ending at Mach 0.75, with output at 0.25-second intervals. Aerothermal convective and radiative indicators are used compute the unmargined aerothermal parameters needed for the thermal model at several body point locations including the nose, nose-cone juncture, shoulder, and afterbody. A fixed HIAD diameter of 6 meters is assumed with a nominal initial roll rate of two revolutions per minute and no initial tip-off rate. Nominally, the initial attitude is targeted to have 0-deg total angle of attach at entry interface of 125 km altitude.

The 2000 trajectories computed in the end-to-end Monte Carlo include 58 uncertainties consisting of mass properties, aerodynamics, and initial entry states, attitude, and roll/tip-off rates. The entry mass is assumed to be known within 1.1% at day of launch, and center-of-gravity location and moments/products of inertia are varied to account for the uncertainty in RV configuration during mass properties

testing. All of the 34 aerodynamic uncertainties are assigned variations heritage of Mars Science Laboratory and other previous missions [6-10]. The initial entry states, attitude, and tip-off rates are varied according to expected uncertainty on the day of launch. The atmosphere is modeled using EarthGRAM 2010 version 4.0, and these variations are handled internally using Markov and wave processes. The sampling process described in Section 3.1 does not currently control these uncertainties in the atmosphere.

3.3 Aerothermodynamic Models and Uncertainties

As noted in the previous subsection, aerothermal forebody convective and radiative indicators are included in POST2 to compute the aerothermal parameters needed for the FTPS thermal model at the nose-cone junction body point near toroid 2. The aerothermal indicators were developed using previous design-cycle trajectories with high-fidelity computational fluid dynamics (CFD) at several points and verified for the trajectory considered in the current design cycle. Two aerothermal parameters, the heat transfer coefficient and radiative heat flux to the vehicle surface, can be tracked from the CFD runs and correlated with curve fits as a function of freestream density, ρ_∞, and velocity, V_∞, as shown in Equations 1 and 2.

$$C_H = k_{CH} * \alpha * \rho_\infty^{\,m} * V_\infty^{\,n} \quad (1)$$

$$q_{rad} = k_{rad} * \alpha * \rho_\infty^{\,m} * V_\infty^{\,n} \quad (2)$$

In Equations 1 and 2, α, m, and n are the curve-fit parameters. A multiplier approach is used to account for the thermochemistry, catalysis, and radiation uncertainties, where the multiplier factors k_{CH} and k_{rad} in Equations 1 and 2, are varied according to the uncertainty information derived from axisymmetric forebody computations for 15 points along 2000 trajectories, given freestream velocity, density, and temperature, from POST2. The Langley Aerothermodynamic Upwind Relaxation Algorithm (LAURA) CFD solver is used to compute the flow field around the forebody surface for a 5-species gas composed of N2, O2, NO, N, and O. HARA is coupled with LAURA to compute the radiative transport to the surface. Five chemical reaction rates [11], 15 collision integrals for the possible species collision pairs [12], catalytic recombination efficiency positive bias of up to 10% above the catalysis model reported by Stewart for outer fabric cloth material [13], and 11 heavy-particle excitation rates for N_2 and NO molecular bands [14] were varied to quantify the uncertainty in the convective heat transfer coefficient and radiative heat flux at the nose-cone juncture body point along the vehicle surface. Given the heat transfer coefficient and radiative heat flux data at this body point, the multiplier coefficient can be computed by comparing (dividing) the CFD-computed values by the aerothermal indicator predictions for each of the 15 trajectory points. The most conservative uncertainty was determined to be at the peak heating trajectory point. A probability distribution fitting algorithm is then used to estimate the statistics for the multiplier data at the peak heating trajectory point. In addition to the two multiplier uncertainties above for the convective and radiative heating indicators on the forebody, a multiplier uncertainty range of -50% to +25% is applied to the convective heating indicator for the aft body points that correspond to the toroid bladders exposed to the wake flow.

3.4 Thermal Models and Uncertainties

A one-dimensional (1-D) physics-based thermal model using COMSOL software is used to obtain the thermal response of the FTPS in the presence of external pressure and aerodynamic heating loads. Heat transfer is modeled within the FTPS layers using several modes including solid conduction, radiation, gas conduction, and advection (i.e., convection within porous material). The amount of heat and mass that is transferred through the FTPS layers is calculated from the solution of the local energy and gas mass conservation equations, which are obtained from the flow theory of gases through a porous solid. The FTPS layup considered for this study consists of two outer fabric layers, three insulation layers, and one gas barrier layer in contact with the toroid 2 skin as shown in **Figure 2** and **Figure 4** (Point 1).

A three-dimensional (3-D) RV thermal model developed in Thermal Desktop solves the thermal response of the toroid IS to the entry heating environment. The physics involved in this model include aeroshell aft-side wake convective heat loads, heat transfer through the toroid skin material, radiation heat transfer within the toroids and between the FTPS and IS, and re-radiation to Earth and Space. The 1-D FTPS and 3-D RV thermal models are coupled by infrared radiation interaction between the FTPS and IS. **Figure 7** illustrates this coupling.

The 1-D FTPS thermal model and 3-D RV thermal model are run sequentially in an iterative fashion to converge on the FTPS/IS interface temperature temporal profile solution. To enable this process, an **effective toroid interior radiation sink temperature** (see **Figure 7**) is calculated from the RV thermal model solution and passed to the FTPS thermal model as the aft-side toroid skin temperature boundary condition.

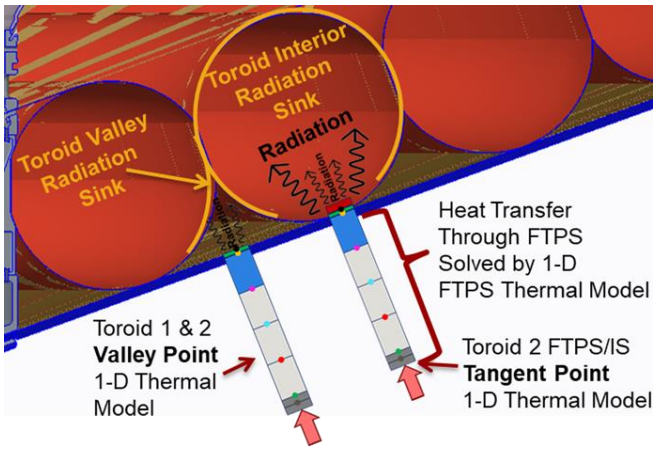

Figure 7. Coupling between the 1-D FTPS/IS Thermal Model and the 3-D Toroid IS Thermal Model

External heat transfer to the FTPS surface is applied according to Equation 3:

$$q_{net} = C_H(H_{0e} - H_w) + q_{rad} - \varepsilon\sigma T_w^4 \quad (3)$$

Here, the 2000 aerothermal parameter temporal profiles, calculated using Equations 1 and 2, are used to compute the transient temperature response dispersions. The wall enthalpy, H_w, is computed using species-dependent enthalpy curve fits from LAURA's thermodynamic database and an assumed wall species composition of 70% N_2, 20% O_2, and 5% NO, by mass. In addition to the 2000 aerothermal parameter temporal profiles, 13 thermal uncertain parameters are varied, including thermal properties (specific heat and thermal conductivity) of the outer fabric and insulation, activation energy for decomposition of the insulation, biases for the outer fabric emissivity, and a maximum interface temperature bias [15-16]. The uncertainties are assigned based on expert opinion and previous testing. Specifically, the maximum interface temperature bias is derived from arc-jet testing to quantify inaccuracies in the model compared to test data due to model-form uncertainties, including FTPS aging and multidimensional effects.

4. RESULTS AND DISCUSSION

Using the end-to-end Monte Carlo uncertainty analysis process, the probability distributions of critical aeroshell thermal responses were calculated. From this information, the risk of aeroshell over-temperature was calculated at critical analysis locations 1 and 2 shown in **Figure 4**. This section will go over the statistical parameters gathered for the FTPS/IS interface and IS toroid skin thermal responses to atmospheric entry.

4.1 IS Toroid Skin Thermal Response Statistics

Figure 8 and **Figure 9** show the results from Monte Carlo #2. Plotted in **Figure 8** is the set of dispersed toroid skin temporal temperature profiles. The data shows that there is a 97.7% probability that the maximum toroid temperature will not exceed 422°C. Furthermore, the calculated risk of exceeding 460°C (T_Allow) is 0%. Therefore, it can be stated that aeroshell is 100% reliable not to exceed the aft-side toroid skin temperature limit. Plotted in **Figure 9** is the set of dispersed effective toroid interior radiation sink temporal temperature profiles. Each sample from this set of profiles is passed into the corresponding sample in Monte Carlo #3 as the aft-side toroid skin temperature radiation sink temperature boundary condition in the FTPS thermal response model. As per the discussion in **Section 2.2,** the performance margin is calculated to be 114°C and the performance margin deficit is -38°C.

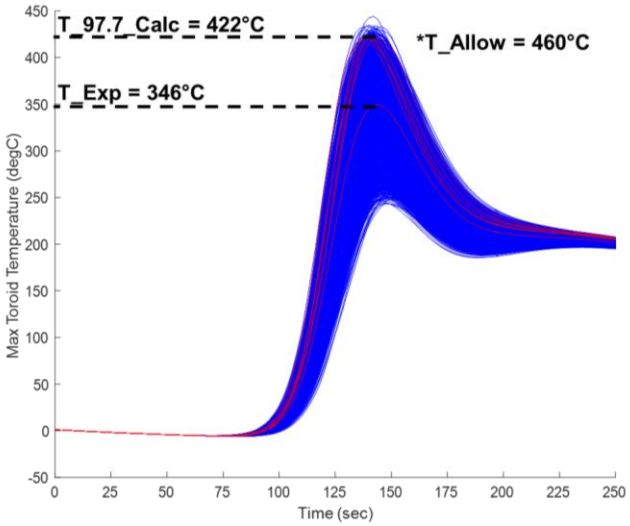

Figure 8. Monte Carlo #2 - Maximum Aft-Side Toroid Skin Temporal Temperature Profile Dispersions

Although the aft-side IS toroids are directly exposed to wake convective heating, the uncertainty analysis shows that there is high confidence that the toroid skin will not exceed fight allowable temperature. In fact, it is over-margined by 38°C as indicated by the negative performance margin deficit. No mitigations are recommended to thermally protect the aft-side IS.

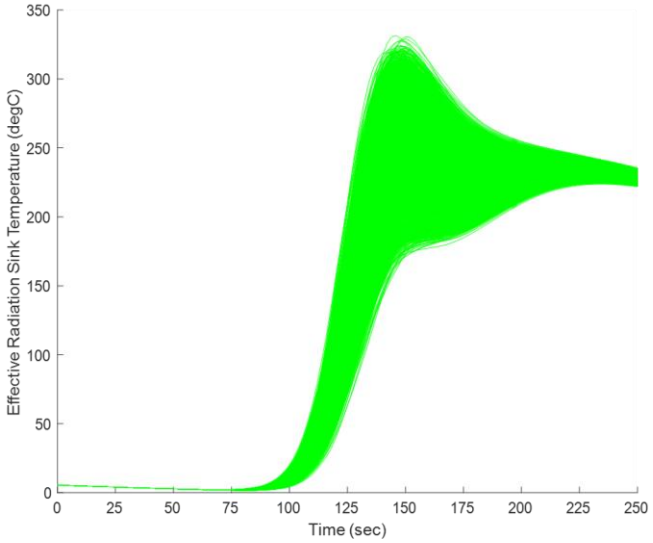

Figure 9. Monte Carlo #2 - Effective Toroid Interior Radiation Sink Temporal Temperature Profile Dispersions

4.2 FTPS/IS Interface Thermal Response Statistics

Figure 10 and **Figure 11** show the results from Monte Carlo #3. **Figure 10** shows that after 2000 samples of the FTPS thermal model are run, the standard deviation has sufficiently converged which indicates a sufficient number of Monte Carlo samples to give accurate statistics.

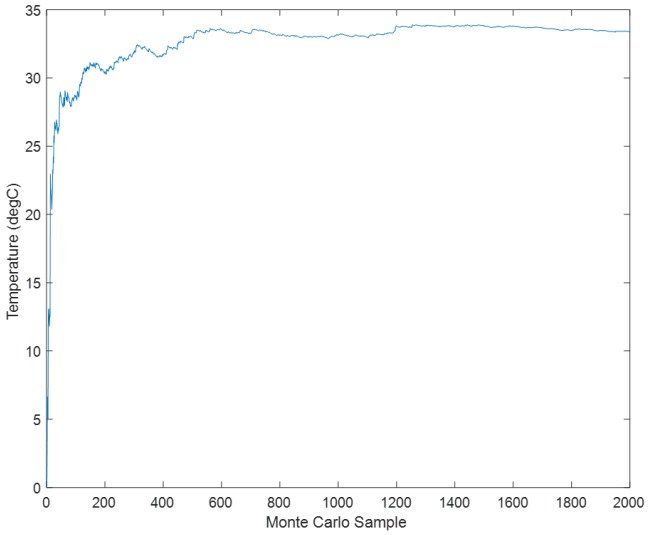

Figure 10. Monte Carlo #3 - Convergence of Maximum FTPS/IS Interface Temperature Standard Deviation

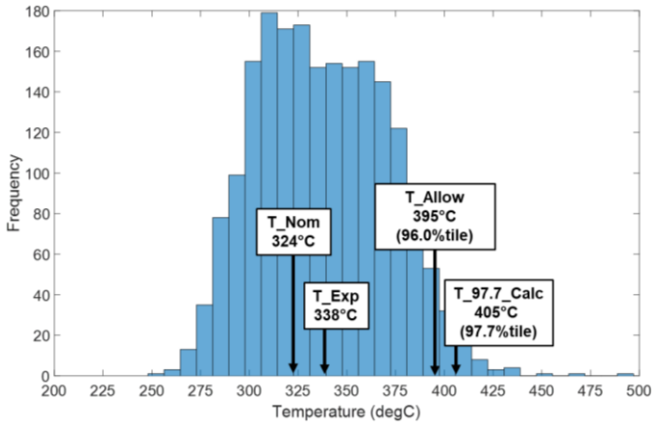

Figure 11. Monte Carlo #3 – 2000 Sample Histogram of Maximum FTPS/IS Interface Temperature

Plotted in **Figure 11** is the histogram of the dispersed maximum FTPS/IS interface temperature. From the statistics supplied by the histogram data, the performance margin is calculated to be 57°C and the performance margin deficit is 10°C. On the histogram plot, it is shown that the 97.7 percentile FTPS/IS interface temperature is 405°C (T_97.7_Calc). **Figure 11** also shows there a 96.0% probability of not-exceeding the flight allowable FTPS/IS interface temperature of 395°C (T_Allow). Therefore, it can be stated that the aeroshell is 96% reliable to survive the planned atmospheric entry.

The calculated FTPS reliability of 96% and performance margin deficit of 10°C indicates that measures should be taken to lower the expected FTPS/IS interface temperature by approximately 10°C. First, it is recommended that adjustments be made to the initial entry state of the trajectory to lower the resultant entry heat load. This can be done by either lowering the initial entry velocity, steepening the entry flight path angle, or some combination of the two. The reliability of the FTPS can also be increased by reducing some of the conservatisms in the thermal models used.

5. CONCLUSIONS

In summary, this paper presented an overview of the probabilistic margin process and how this informs the necessary design changes needed to meet the reliability standard for LOFTID. The uncertainty analysis shows that there is high confidence that the aft-side toroid skin, subject to wake convective heat loads, will not exceed fight allowable temperatures. However, the uncertainty analysis also showed that the aeroshell is 96% reliable to survive atmospheric entry based on the calculated probability of the FTPS/IS interface exceeding its flight allowable temperature. As such, the current risk of aeroshell failure falls short of satisfying the project's reliability standard. Therefore, mitigation is

recommended to make adjustments to the entry trajectory, reduce conservatisms in the thermal models, or a combination thereof. Although this paper focuses on the application of the probabilistic margin process for the HIAD thermal protection system, this methodology can also be applicable to other entry systems and related engineering disciplines.

6. REFERENCES

[1] Tobin, S. A. and Dec, J. A., "A Probabilistic Sizing Demonstration of a Flexible Thermal Protection System for a Hypersonic Inflatable Aerodynamic Decelerator," AIAA Paper 2015-1895.

[2] Dec, J. A. and Mitcheltree, R. A., "Probabilistic Design of A Mars Sample Return Entry Vehicle Thermal Protection System," AIAA Paper 2002-0910.

[3] Cozmuta, I., Wright, M., J., Laub, B., Willcockson, W., H., "Defining Ablative Thermal Protection System Margins for Planetary Entry Vehicles," 42nd AIAA Thermophysics Conference, AIAA 2011-3757, Honolulu, Hawaii, June 2011.

[4] Wright, M. J., Bose, D., and Chen, Y.-K., "Probabilistic Modeling of Aerothermal and Thermal Protection Material Response Uncertainties," AIAA Journal, Vol. 45, No. 2, 2007, pp. 399-410. doi: 10.2514/1.26018.

[5] Iman, R. L., and Shortencarier, M. J., "A Fortran 77 Program and User's Guide for the Generation of Latin Hypercube and Random Samples for Use with Computer Models," NUREG/CR-3624, Technical Report SAND83-2365, Sandia National Laboratories, Albuquerque, NM, 1984.

[6] Gnoffo, P. A., Braun, R. D., Weilmuenster, K. J., Mitcheltree, R. A., Engelund, W. C., Powell, R. W., "Prediction and Validation of Mars Pathfinder Hypersonic Aerodynamic Database", Journal of Spacecraft and Rockets, Vol. 36, No. 3, May-Jun 1999, pp. 367-373.

[7] Olds, A. D., Beck, R. E., Bose, D. M., White, J. P., Edquist, K. T., Hollis, B. R., Lindell, M. C., Cheatwood, F. M., "IRVE-3 Post-Flight Reconstruction", AIAA 2013-1390, March 2013.

[8] Schoenenberger, M., Van Norman, J. W., Karlgaard, C., Kutty, P., Way, D., "Assessment of the Reconstructed Aerodynamics of the Mars Science Laboratory Entry Vehicle", Journal of Spacecraft and Rockets, Vol. 51, No. 4, Jul-Aug 2014, pp. 1076-1093.

[9] Moss, J. N., Glass, C. E., Hollis, B. R., Van Norman, J. W., "Low-Density Aerodynamics for the Inflatable Reentry Vehicle Experiment", Journal of Spacecraft and Rockets, Vol. 43, No. 6, Nov-Dec 2006, pp. 1191-1201.

[10] Edquist, K. T., Desai, P. N., Schoenenberger, M., "Aerodynamics for Mars Phoenix Entry Capsule", Journal of Spacecraft and Rockets", Vol. 48, No. 5, Sept-Oct 2011, pp. 713-726.

[11] West, T. and Johnston, C. O., "Uncertainty and Sensitivity Analysis of Afterbody Radiative Heating Predictions for Earth Entry", Journal of Thermophysics and Heat Transfer, Vol. 31, No. 2 (2017), pp. 294-306.

[12] Wright, M., Bose, D., Palmer, G., and Levin, E., "Recommended Collision Integrals for Transport Property Computations Part 1: Air Species", AIAA Journal, Vol. 43, No. 12 (2005), pp. 2558-2564.

[13] Stewart, D., "Determination of Surface Catalytic Efficiency for Thermal Protection Materials – Room Temperature to Their Upper Use Limit", AIAA 1996-1863, 31st Thermophysics Conference, Fluid Dynamics and Co-located Conferences.

[14] Johnston, C. O., private communication, 2018-03-13

[15] Rossman, G. A., "Conceptual Thermal Response Modeling, Testing, and Design of Flexible Heatshield Insulation Material", Thesis, Gerogia Institute of Technology, 2017

[16] Tobin, S. A. and Dec, J. A., "A Probabilistic Sizing Demonstration of a Flexible Thermal Protection System for a Hypersonic Inflatable Aerodynamic Decelerator", AIAA 2015-1895, 53rd AIAA Aerospace Sciences Meeting, Jan. 2015